Electrochemical characterization of insulating silica-modified electrodes: transport properties and physicochemical features

Valentina Pifferi[a,b,*], Luca Rimoldi[a,b,*], Daniela Meroni[a,b,*], Francesco Segrado[a], Guido Soliveri[c], Silvia Ardizzone[a,b], Luigi Falciola[a,b]

[a] *Dipartimento di Chimica, Università degli Studi di Milano, Via Golgi 19, 20133 Milano, Italy*

[b] *Consorzio Interuniversitario Nazionale per la Scienza e la Tecnologia dei Materiali (INSTM), Via Giusti 9, 50121 Firenze, Italy*

[c] *Department of Engineering Physics, Polytechnique Montréal, H3T 1J4 Montreal, Canada*

* *Corresponding authors:* luca.rimoldi@unimi.it; valentina.pifferi@unimi.it; daniela.meroni@unimi.it

Abstract

The role played by the deposition of subsequent insulating layers from a silica sol onto an ITO support was investigated to elucidate the modifications occurring to diffusion and transfer mechanisms with respect to bare electrodes. The electrochemical characterization highlighted peculiar trends, which were discussed with respect to literature models and interpreted on the grounds of the physicochemical characterizations (FE-SEM, AFM, UV-vis transmittance) and mainly of the layers hydrophilicity.

Keywords

Electroinactive layer; blocked electrode; wettability; transport properties; diffusion coefficient; redox probe

1. Introduction

The modification of electrodes by deposition of electroinactive layers (*e.g.* insulating oxides or non-conductive polymers), in which analytes can dissolve and diffuse, is a field of great interest for electrochemical (fuel cells, batteries, …) and electroanalytical (sensors) applications due to the possibility to tune diffusion, transport and reactivity properties [1–5]. Starting from the pioneering works by Gileadi *et al.* and Amatore *et al.* about partially blocked electrodes [6,7], theoretical and computational models have been proposed to rationalize these phenomena [1,4,8–11]. However,

experimental studies aiming at verifying such theoretical models have been scarce [12,13]. Furthermore, the inactive layer morphology and physicochemical features have been often disregarded in the complete understanding of the electrochemical performance. In this context, the development of electrodes modified with tailored electroinactive layers is crucial to clarify the mechanisms of diffusion, mass transport and charge transfer in these systems.

In the present work, planar ITO-coated glass electrodes were modified by the deposition of a silica sol and the role of film thickness was studied by depositing subsequent layers. The modified electrodes were characterized by field emission scanning electron microscopy (FE-SEM), atomic force microscopy (AFM), UV-vis transmittance and water contact angle measurements to investigate their morphological and physicochemical properties. Electrochemical measurements by both cyclic voltammetry (CV) and electrochemical impedance spectroscopy (EIS), adopting both negatively and positively charged electrochemical probes, allowed diffusion and transport phenomena to the electrode to be understood.

2. Experimental section

2.1 Samples preparation

Indium tin oxide (ITO) supports (Sigma-Aldrich, 15-25 Ω-sq^{-1}, 2.5 × 2 cm^2) were used as substrates for film deposition. Before deposition, they were sonicated in a water/isopropanol (50:50) mixture and in water, then dipped in H_2SO_4 98% for 30 s, rinsed with water and dried under N_2 flux.

A silica sol was prepared by mixing 16.8 mL of water, 25.4 mL of ethanol, 2.2 mL of HCl 1 M and 4.9 mL of tetraethyl orthosilicate. The sol was stirred for 1 h, then aged at room temperature for 24 h before use.

Silica films were prepared by spin coating the silica sol (3000 rpm, 30 s, 500 rpm s^{-1}) on the cleaned ITO glass, repeating the deposition procedure up to 5 times to obtain multilayers. Each layer was ca. 100 nm-thick, as determined by FE-SEM cross sectional images. Finally, films were dried at room temperature overnight. Each film was re-synthesized at least 3 times. Samples were labelled "SiO_2_n", where *n* is the number of deposited silica layers.

2.2 Materials characterization

FE-SEM images were obtained on pristine films on a Zeiss Supra 40 working in high vacuum and equipped with a GEMINI column,with a high efficiency In-lens detector. Elecron energy: 200 V – 30 kV. Max resolution: 1 nm @ 20kV (detector In-lens).

AFM measurements were performed on a FastScan (Bruker) microscope working in tapping mode. Root mean squared roughness (RMS) values were obtained on 1 × 1 μm^2 areas.

The average dimension of colloidal nuclei of the silica sol was measured by dynamic light scattering (DLS) using a Malvern Zetasizer Nano ZS.

UV-vis transmittance spectra were recorded on a Shimadzu UV2600 spectrophotometer.

Wetting properties of silica films were evaluated by static and dynamic contact angle measurements (Krüss EasyDrop) on at least 5 different spots.

The electrochemical characterization was performed in a three-electrode cell (RE: saturated calomel, CE: Pt wire, WE: modified ITO glass) using a PGstat30 potentiostat/galvanostat (Autolab, The Netherlands), equipped with a FRA module. KCl 0.1 M was used as supporting electrolyte and 3 mM $[Fe(CN)_6]^{4-}/[Fe(CN)_6]^{3-}$ or $[Ru(NH_3)_6]^{3+}/[Ru(NH_3)_6]^{2+}$ as redox probes. Solutions were prepared using doubly distilled water (conductivity: 18 μS cm^{-1}) purified by a MilliQ apparatus. The electrochemical cell was not deaerated and worked at room temperature. CV parameters were the following: step potential 0.005 V, scan rate range 0.01-0.75 V s^{-1}. EIS parameters were the following: frequency range 0.1-65000 Hz, amplitude 0.01 V. Impedance data were elaborated by Z-view 3.1 software. Each sample was tested several times, in a time interval of several months, showing no appreciable modifications.

3. Results and discussion

3.1 Morphological properties

FE-SEM images show that all samples exhibited high homogeneity and complete substrate coverage (Fig. 1a), with a morphology characterized by nanometric silica domains (Fig. 1a, inset), with no significance differences regarding the number of the deposited layers. The nanometric features at the film surface can be traced back to the colloidal silica sol: DLS measurements performed on the sol before deposition show that the transparent hydroalcoholic solution contained silica nuclei of ca. 5 ± 2 nm size (Fig. 1b). The homogeneity of the silica films was confirmed by AFM images (Fig. 1c), showing low surface roughness (RMS for SiO_2_1: 0.7 nm).

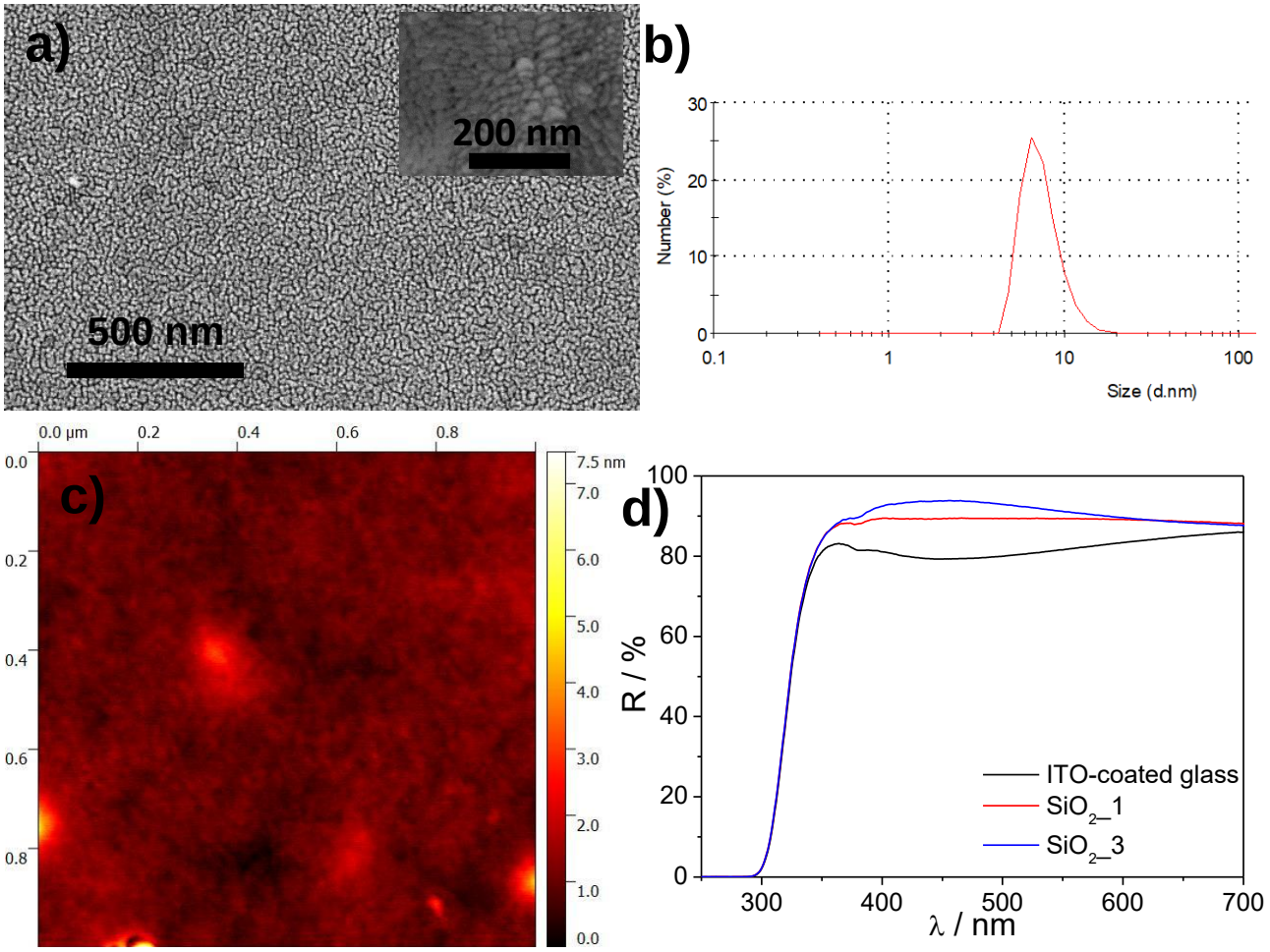

Figure 1 – FE-SEM images (magnification in inset) of the SiO_2_3 sample (a); DLS analysis of the silica sol (b); AFM picture of the SiO_2_1 sample (c); UV-vis transmittance spectra of modified and unmodified electrodes (d).

The optical properties of the silica films were studied by UV-vis transmittance spectroscopy. The ITO-coated glass shows a typical spectrum characterized by an absorption edge at about 320 nm. The deposition of silica sol does not shift the absorption edge of the films. However, with respect to the ITO-coated substrate, the silica coated samples exhibit higher transmittance in the 350-600 nm region due to the larger refractive index of ITO with respect to SiO_2 (Fig. 1d). Successive depositions of SiO_2 further increase the optical transparency, consistently with the formation of a thicker homogeneous anti-reflective layer.

The wetting properties of the different samples were investigated measuring water contact angles, θ_w [14]. While ITO is hydrophobic (θ_w ca. 90°) with a moderate hysteresis between advancing and receding angles (ca. 30°), all silica modified electrodes are characterized by lower θ_w, *i.e.* a higher hydrophilicity, and by a large hysteresis between advancing and receding angles (hysteresis starting from 55 and up to 69° for the different samples), compatible with a Wenzel state [15,16]. SiO_2_3

shows a lower value of θ_w as an evidence of an appreciably increased hydrophilic character of the electrode (Tab. 1, 2nd column). Contact angle values further decrease for successive depositions, reaching about 40° with 5 layers. This latter effect can be interpreted as due to the increased water chemisorption ensuing the growth of the film nanostructure with its thickness, as proposed by Ganesh *et al.* for TiO_2 layers [17].

Sample	**Wettability**	**Electrochemical characterization**				
	Static contact angle	CV Fe probe		CV Ru probe		EIS
	θ_w / °	Slope i_a *vs* $v^{0.5}$ / (mA cm^{-2} $V^{-0.5}$ $s^{0.5}$)	Slope ln i_a *vs.* ln *v*	Slope i_c *vs* $v^{0.5}$ / (mA cm^{-2} $V^{-0.5}$ $s^{0.5}$)	Slope ln i_c *vs.* ln *v*	R_{CT} / (kΩ cm^2)
ITO	90	2.16 ± 0.08	0.50 ± 0.01	- 1.30 ± 0.02	0.45 ± 0.01	-
SiO_2_1	76	(2.14 ± 0.03) · 10^{-2}	0.31 ± 0.01	(- 7.3 ± 0.2) · 10^{-2}	0.28 ± 0.02	29 ± 3
SiO_2_2	69	(0.48 ± 0.04) · 10^{-2}	0.18 ± 0.03	(- 1.07 ± 0.03) · 10^{-2}	0.21 ± 0.02	71 ± 1
SiO_2_3	51	(7.94 ± 0.09) · 10^{-2}	0.36 ± 0.01	(- 18.0 ± 0.3) · 10^{-2}	0.36 ± 0.02	6.6 ± 0.1

Table 1 –Static water contact angles (± 5°), CV parameters for both electrochemical probes, and charge transfer resistances, R_{CT}, retrieved by EIS measurements.

3.2 Electrochemical properties

CV and EIS were employed with two commonly adopted redox probes: $[Fe(CN)_6]^{4-}$/$[Fe(CN)_6]^{3-}$ and $[Ru(NH_3)_6]^{3+}$/$[Ru(NH_3)_6]^{2+}$, which present the same dimensions being different by their opposite charge [18–20]. Therefore, the two probes are supposed to behave differently with respect to SiO_2, which is negatively charged in the working conditions (pH 5 – 6 aqueous KCl solution), having an isoelectric point very close to 3 [21,22].

The deposition of SiO_2 layers on ITO drastically decreases the probes electrochemical response in comparison with the bare support (Tab. 1), due to the insulating properties of the oxide, confirming the homogeneity and complete coverage found by FE-SEM characterization. The present electrodes can be considered non-porous electroinactive materials as the measured electrochemical response can be ascribed to the diffusion of the active species through the material. The current decrease, by about one order of magnitude with respect to ITO, is more evident in the case of the negatively charged iron probe, as expected by the charge repulsion from SiO_2. However, the study of SiO_2_n samples revealed an unexpected behaviour with both probes: while the peak current decreases passing from one to two insulating layers, we observed an unforeseen increase when the third layer is added (Fig. 2a,b). Moreover, the voltammogram shape undergoes a remarkable change during the layer transition, which is dependent on the scan rate. In particular, in the case of SiO_2_1 (curve A), the voltammogram presents a quasi-step shape for low scan rates (Fig. 2a) transforming in a peak for higher scan rates (not shown). When two SiO_2 layers are deposited (SiO_2_2, curve B), a step is

obtained for the entire scan rate range. The addition of a third layer (SiO_2_3, curve C) always results in a peak-shaped voltammogram, regardless of the scan rate. The deposition of further layers increases the capacitive currents and the background noise for the insulating properties of silica, making the probes undetectable (curve D).

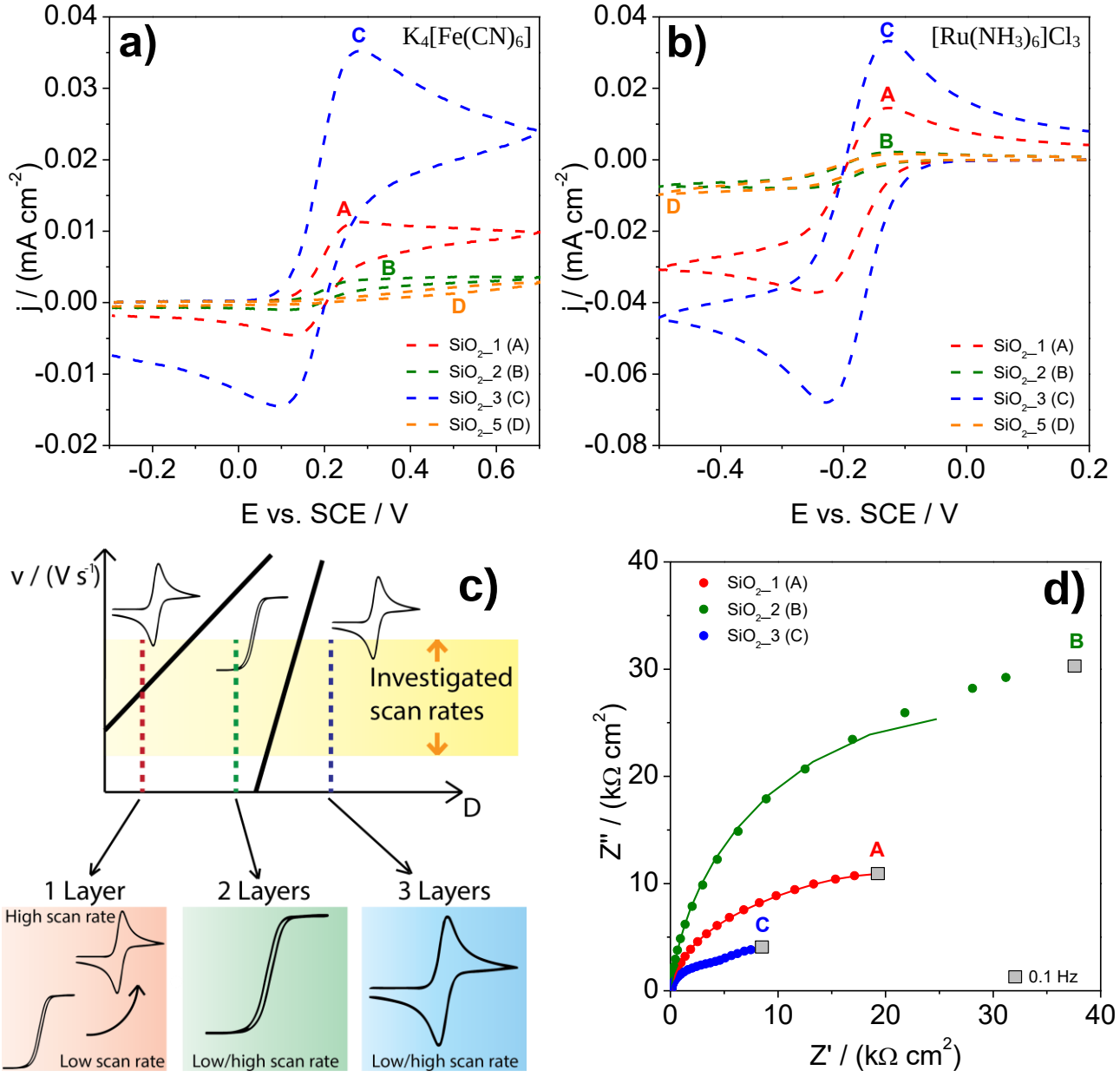

Figure 2 – Cyclic voltammograms registered at 100 mV s^{-1} for electrodes modified with different layers of silica in the presence of 3 mM (a) $K_4[Fe(CN)_6]$ and (b) $[Ru(NH_3)_6]Cl_3$. Schematic representation of the CV pattern evolution according to Compton's theoretical model: adapted from ref. [1] (c). Complex plane plot in the presence of 3 mM $K_4[Fe(CN)_6]$ registered at + 0.25 V (d).

This trend is confirmed by the slopes obtained from the Randles-Sevčik plot (Tab. 1, 3rd – 5th columns). Furthermore, the very low slope values (<< 0.5) of ln *i* *vs.* ln *v* plots for all silica samples

(Tab. 1, 4^{th} – 6^{th} columns), support the evidence of a remarkable modification of the probe diffusion mode, which cannot be described anymore only by the classical planar diffusion phenomenon [1].

Furthermore, EIS measurements (Fig. 2d) show that the highest and the lowest impedance values are observed for the 2 and 3 layers samples, respectively. Also the charge transfer resistance values, obtained by the fitting of impedance data (Tab. 1, 7^{th} column), follow the same trend.

The characteristic electrochemical behaviour shown by the SiO_2_n samples can be examined on the grounds of literature results relative to simulated voltammetric patterns, theorized by Compton *et al.* for non-porous electroinactive materials [1,4]. Compton *et al.* ascribed the different shapes of the voltammetric response to the change of probe diffusion coefficient inside the insulating layer in comparison with that of the bulk solution (Fig. 2c) [1]. According to their simulations, under the adopted experimental conditions, a transition from step-shaped to peak-shaped voltammograms by increasing the scan rate should be recorded (Fig. 2c, red line) considering the conventional diffusion coefficients of the two probes in solution. Actually, this behaviour was found only for SiO_2_1. An increase of the material diffusion coefficient must be invoked when only step-shaped voltammograms are recorded in the investigated scan rate range (Fig. 2c, green line). This corresponds, in the present case, to SiO_2_2. Moreover, peak-shaped voltammograms independent of scan rate may be due to a further increase of the diffusion coefficients in the insulating layer (Fig. 2c, blue line). This might mirror the behaviour of SiO_2_3. Therefore, an increase of the diffusion coefficient with layers in the silica-based electrodes should be invoked.

The overall electrochemical behaviour shown by the present layers are closely related to the physicochemical features of the electrode [4,23]. The apparent diffusion coefficient increase with the number of silica layers, together with the observed peak current behaviour (Fig. 2a,b), can be the result of a complex balance between diverging effects. The progressive decrease in water contact angle of the layers produces a higher affinity between the electrolyte solution and the electrode surface, with an ensuing promotion of the diffusion coefficient. On the other hand, the silica insulating properties cause competing detrimental effects on the electrochemical performance with increasing film thickness. The optimal balance of these two diverging effects was found in the present case for SiO_2_3, which shows the highest peak current density and the lowest impedance values.

4. Conclusions

The consecutive deposition of insulating silica layers onto an ITO electrode was analysed with the aim of providing experimental evidence to theoretical models concerning electroinactive layer-

modified electrodes. Both FE-SEM, AFM and UV-vis spectroscopy show that the conductive support is covered by a continuous and homogeneous layer. The electrochemical characterizations revealed a scan rate-dependent variation of the CV shape with the number of insulating layers, which was attributed, on the grounds of previous theoretical models, to a progressive increase of the diffusion coefficient. In the present case, the progressive enhancement of film hydrophilicity is proposed as a possible origin of this diffusion coefficient increase. The balance between the diffusion coefficient increase and the insulating effect produced by consecutive silica layer addition, is proposed to interpret the overall electrochemical behaviour. The present results can offer an interpretative framework to better understand diffusion and transport properties in a number of electroinactive layer-modified electrodes, such as sensors, batteries and fuel cells.

References

[1] D. Menshykau, R.G. Compton, Electrodes Modified with Electroinactive Layers: Distinguishing Through-Film Transport from Pinhole (Pore) Diffusion, Langmuir. 25 (2009) 2519–2529. doi:10.1021/la803488t.

[2] G. Giordano, C. Durante, A. Gennaro, M. Guglielmi, Multilayer Deposition of Silica Sol–Gel Films by Electrochemical Assisted Techniques, J. Phys. Chem. C. 120 (2016) 28820–28824. doi:10.1021/acs.jpcc.6b10040.

[3] C. Song, G. Villemure, Electrode modification with spin-coated films of mesoporous molecular sieve silicas, Microporous Mesoporous Mater. 44–45 (2001) 679–689. doi:10.1016/S1387-1811(01)00249-9.

[4] S. Eloul, C. Batchelor-McAuley, R.G. Compton, Thin film-modified electrodes: a model for the charge transfer resistance in electrochemical impedance spectroscopy, J. Solid State Electrochem. 18 (2014) 3239–3243. doi:10.1007/s10008-014-2662-1.

[5] M. Saadaoui, I. Fernández, G. Luna, P. Díez, S. Campuzano, N. Raouafi, et al., Label-free electrochemical genosensor based on mesoporous silica thin film, Anal. Bioanal. Chem. 408 (2016) 7321–7327. doi:10.1007/s00216-016-9608-7.

[6] H. Reller, F. Kirowa-Eisner, E. Gileadi, Ensembles of microelectrodes: A digital-simulation, J. Electroanal. Chem. Interfacial Electrochem. 138 (1982) 65–77. doi:10.1016/0022-0728(82)87128-3.

[7] C. Amatore, J.M. Savéant, D. Tessier, Charge transfer at partially blocked surfaces, J.

Electroanal. Chem. Interfacial Electrochem. 147 (1983) 39–51. doi:10.1016/S0022-0728(83)80055-2.

[8] K. Neyts, M. Karvar, O. Drobchak, T. Brans, F. Strubbe, F. Beunis, Simulation of charge transport and steady state in non-polar media between planar electrodes with insulating layers, Colloids Surfaces A Physicochem. Eng. Asp. 440 (2014) 101–109. doi:10.1016/j.colsurfa.2012.10.022.

[9] F.G. Chevallier, N. Fietkau, J. del Campo, R. Mas, F.X. Muñoz, L. Jiang, et al., Experimental cyclic voltammetry at partially blocked electrodes: Elevated cylindrical blocks, J. Electroanal. Chem. 596 (2006) 25–32. doi:10.1016/j.jelechem.2006.06.015.

[10] F.G. Chevallier, T.J. Davies, O. V. Klymenko, L. Jiang, T.G.J. Jones, R.G. Compton, Influence of the block geometry on the voltammetric response of partially blocked electrodes: Application to interfacial liquid–liquid kinetics of aqueous vitamin B12S with random arrays of femtolitre microdroplets of dibromocyclohexane, J. Electroanal. Chem. 580 (2005) 265–274. doi:10.1016/j.jelechem.2005.03.036.

[11] F.G. Chevallier, T.J. Davies, O. V. Klymenko, L. Jiang, T.G.J. Jones, R.G. Compton, Numerical simulation of partially blocked electrodes under cyclic voltammetry conditions: influence of the block unit geometry on the global electrochemical properties, J. Electroanal. Chem. 577 (2005) 211–221. doi:10.1016/j.jelechem.2004.11.033.

[12] A. Walcarius, E. Sibottier, M. Etienne, J. Ghanbaja, Electrochemically assisted self-assembly of mesoporous silica thin films, Nat. Mater. 6 (2007) 602–608. doi:10.1038/nmat1951.

[13] A. Vuorema, M. Sillanpää, K.J. Edler, R. Jaber, S.E.C. Dale, S. Bending, et al., Mesoporous Silica Sputter-Coated onto ITO: Electrochemical Processes, Ion Permeability, and Gold Deposition Through NanoPores, Electroanalysis. 24 (2012) 1296–1305. doi:10.1002/elan.201200141.

[14] G. Soliveri, V. Pifferi, R. Annunziata, L. Rimoldi, V. Aina, G. Cerrato, et al., Alkylsilane–SiO_2 Hybrids. A Concerted Picture of Temperature Effects in Vapor Phase Functionalization, J. Phys. Chem. C. 119 (2015) 15390–15400. doi:10.1021/acs.jpcc.5b04048.

[15] D. Quéré, Wetting and Roughness, Annu. Rev. Mater. Res. 38 (2008) 71–99. doi:10.1146/annurev.matsci.38.060407.132434.

[16] D. Meroni, S. Ardizzone, G. Cappelletti, M. Ceotto, M. Ratti, R. Annunziata, et al., Interplay between Chemistry and Texture in Hydrophobic TiO_2 Hybrids, J. Phys. Chem. C. 115 (2011)

18649–18658. doi:10.1021/jp205142b.

[17] V.A. Ganesh, A. S. Nair, H.K. Raut, T.M. Walsh, S. Ramakrishna, Photocatalytic superhydrophilic TiO_2 coating on glass by electrospinning, RSC Adv. 2 (2012) 2067. doi:10.1039/c2ra00921h.

[18] V. Pifferi, M.M. Barsan, M.E. Ghica, L. Falciola, C.M.A. Brett, Synthesis, characterization and influence of poly(brilliant green) on the performance of different electrode architectures based on carbon nanotubes and poly(3,4-ethylenedioxythiophene), Electrochim. Acta. 98 (2013) 199–207. doi:10.1016/j.electacta.2013.03.048.

[19] V. Pifferi, G. Cappelletti, C. Di Bari, D. Meroni, F. Spadavecchia, L. Falciola, Multi-Walled Carbon Nanotubes (MWCNTs) modified electrodes: Effect of purification and functionalization on the electroanalytical performances, Electrochim. Acta. 146 (2014) 403–410. doi:10.1016/j.electacta.2014.09.099.

[20] T. Doneux, A. de Ghellinck, E. Triffaux, N. Brouette, M. Sferrazza, C. Buess-Herman, Electron Transfer Across an Antifouling Mercapto-hepta(ethylene glycol) Self-Assembled Monolayer, J. Phys. Chem. C. 120 (2016) 15915–15922. doi:10.1021/acs.jpcc.5b12260.

[21] S. Schwarz, K. Lunkwitz, B. Keßler, U. Spiegler, E. Killmann, W. Jaeger, Adsorption and stability of colloidal silica, Colloids Surfaces A Physicochem. Eng. Asp. 163 (2000) 17–27. doi:10.1016/S0927-7757(99)00426-4.

[22] M. Kosmulski, A literature survey of the differences between the reported isoelectric points and their discussion, Colloids Surfaces A Physicochem. Eng. Asp. 222 (2003) 113–118. doi:10.1016/S0927-7757(03)00240-1.

[23] M.E. Orazem, B. Tribollet, Electrochemical Impedance Spectroscopy, John Wiley & Sons, Inc., Hoboken, NJ, USA, 2008. doi:10.1002/9780470381588.